Photodetachment Spectroscopy of Negative Cluster Ions.

S. T. ARNOLD, J. V. COE (a), J. G. EATON, C. B. FREIDHOFF (b), L. KIDDER, G. H. LEE (c), M. R. MANAA, K. M. MCHUGH (d), D. PATEL-MISRA, H. W. SARKAS, J. T. SNODGRASS (e) and K. H. BOWEN (*)

Department of Chemistry, 34th and Charles Streets, The Johns Hopkins University Baltimore, MD 21218

1. – Introduction.

The study of gas phase cluster anions provides an avenue for addressing open questions in topics as diverse as ion solvation, excess electrons in fluids, ion-molecule reactions, ion-induced nucleation, chemisorption on surfaces and electronic band structure in solids. In the past, experimental investigations of negative cluster ions have included thermochemical [1-3], kinetic [4], electron attachment [5, 6] and spectroscopic studies, with the latter exploring total photodestruction [7, 8], photodissociation [9, 10] and photodetachment [11] processes. At the same time, theoretical studies have dealt with the related topics of negative-ion solvation [12-14], trapped and solvated electron states [15, 16] and the variation of metal cluster electron affinities with cluster size [17-19].

The photodetachment of electrons from mass-selected cluster anions yields incisive information not only about individual sizes of cluster anions but also about their corresponding neutral clusters. When these experiments are conducted as a function of cluster size, it becomes possible to monitor the evolution of several important properties from those of single atomic or molecular species toward those of the condensed phase. In recent years, dramatic progress in the photodetachment of negative cluster ions and related

(a) Present address: Department of Chemistry, Ohio State University, Columbus OH 43210.
(b) Present address: Westinghouse Research and Development Center, Pittsburgh, PA.
(c) Present address: Department of Chemistry, Columbia University, New York, NY 10927.
(d) Present address: National Engineering Laboratory, Idaho Falls, ID.
(e) Present address: American Cyanamid Company, Princeton, NJ 08543-0400.
(*) Author to whom correspondence should be addressed.

species has been occurring in several laboratories. Using pulsed negative-ion photoelectron spectroscopy, SMALLEY and his colleagues [20-27] have recorded the spectra of $C^-_{n=2\div30,48\div84}$, $Cu^-_{n=6\div41}$, $Ag^-_{n=3\div21}$, $Au^-_{n=2\div21}$, $Nb^-_{n=4\div12}$, $Pb^-_{n=2\div12}$, $Si^-_{n=3\div20}$, $Ge^-_{n=3\div15}$, $Sn^-_{n=2\div12}$ and $Al^-_{n=3\div32}$; Johnson's group [28-31] has measured the spectra of $(O_2)^-_{n=2\div6}$, $O_2^-(N_2)_1$, $NO^-(NO)_1$, $(CO_2)^-_{n=2\div13}$, $O_2^-(H_2O)_1$ and $NO_2^-(N_2O)_1$; NEUMARK *et al.* [32-34] have recorded the spectra of $(ClHCl)^-$, $(IHI)^-$, $(BrHBr)^-$, $(FHCl)^-$ and $(BrHCl)^-$; and MEIWES-BROER and his colleagues [35, 36] have taken the spectra of $Al^-_{n=3\div14}$, $Ag^-_{n=3\div22}$ and $Ni^-_{n=2\div18}$. Using ion cyclotron resonance photodetachment spectroscopy, BRAUMAN *et al.* [37-39] have recorded the spectra of a variety of solvated anions of the form $ROHF^-$. Using c.w. negative-ion photoelectron spectroscopy, Lineberger's group [40-48] has measured the spectra of $Cu^-_{n=2\div10}$, Fe_2^-, Co_2^-, $Ag^-_{n=2\div6}$, Re_2^-, $Ni^-_{n=2\div8}$, Pd_3^-, $Pt^-_{n=2,3}$, $(Na_mF_n)^-$, $Fe(CO)^-_{n=1\div4}$, $Ni(CO)^-_{n=1\div3}$ and $H^-(H_2O)_1$; ELLISON *et al.* [49] have taken the spectrum of Si_2^-; and in our laboratory [50-54] we have recorded the photoelectron spectra of $NO^-(N_2O)_{n=1\div5}$, $H^-(NH_3)_{n=1,2}$, $D^-(ND_3)_1$, $NH_2^-(NH_3)_{n=1,2}$, $ND_2^-(ND_3)_{n=1,2}$, $NO^-(Ar)_1$, $NO^-(Kr)_1$, $NO^-(Xe)_1$, $O_2^-(Ar)_1$, $NO^-(H_2O)_{n=1,2}$, $NO^-(D_2O)_{n=1,2}$, $(CO_2)_2^-$, $(N_2O)_2^-$, $(CS_2)_2^-$, $(SO_2)_2^-$, $(H_2O)^-_{n=2,6,7,10\div25,30,34,37,40}$, $(D_2O)^-_{n=2,6,7,11\div23}$, $Ar(H_2O)^-_{n=2,6,7}$, $Ar(D_2O)^-_{n=2,6,7}$, $Ar_2(D_2O)_6^-$, $Na^-_{n=2\div5,7}$, $K^-_{n=2\div8}$, $Rb^-_{n=2\div4}$, $Cs^-_{n=2,3}$, $(NaK)^-$, $(Na_2K)^-$, $(KRb)^-$, $(KCs)^-$, $(K_2Cs)^-$ and $(RbCs)^-$. Clearly, progress in cluster anion photodetachment spectroscopy has been rapid, and the field is beginning to flourish across a chemically diverse range of systems.

Here, we provide a summary of our work in this area. Our goals in studying the photodetachment of negative cluster ions are 1) to explore their energetic properties as a function of cluster size and 2) to develop a descriptive understanding of the bonding within negative cluster ions. Important energetic properties include electron affinities and stepwise ion-solvent dissociation (solvation) energies. Clustering can be expected to stabilize the excess charge on negative ions. One also expects that electron affinity values will increase rapidly with cluster size for small clusters and then approach a limiting value at some larger size as the mean number of solvent molecules interacting with the anion becomes constant. Stepwise solvation energies should eventually decrease with increasing solvation numbers. The experiments reported here map out both electron affinities and stepwise solvation energies as a function of cluster size.

An important aspect of ion-neutral bonding concerns the distribution of excess negative charge over the negative cluster ion. One can imagine two extreme charge distribution categories, where in one the excess charge is localized on a single component of the cluster ion, and where in the other there is a dispersal of the negative charge over part or all of the cluster ion. The situation where the excess charge is localized on a single component of the cluster ion is reminiscent of the usual notion of a solvated anion in which a central negative ion is surrounded by a sheath of neutral solvent molecules. There the central negative ion may be thought of as remaining largely intact even though it is

perturbed by its solvents. In this case electrostatic interactions between the ion and the solvent molecules presumably dominate the bonding. In other cases, however, charge dispersal effects may also make significant contributions to the bonding. These contributions may arise either in the sense of covalency in ion-neutral bonds or in the sense of excess electron delocalization via electron tunneling between energetically and structurally equivalent sites within the cluster ion. In favorable cases the photoelectron spectra of negative cluster ions can offer clues as to the nature of the excess charge distribution in these species.

In this lecture the results are organized into two parts: 1) ion-molecule complexes where the excess electron is localized on one component of the negative cluster ion and 2) more complicated cluster anions involving significant excess negative-charge dispersal. The spectra of $NO^-(N_2O)_{n=1\div5}$, $H^-(NH_3)_{n=1,2}$, $NH_2^-(NH_3)_{n=1,2}$, $NO^-(Ar)_1$, $NO^-(Kr)_1$, $NO^-(Xe)_1$, $NO^-(H_2O)_{n=1,2}$, $O_2^-(Ar)_1$, $(N_2O)_2^-$ and $(CS_2)_2^-$ reveal that they are relatively simple ion-molecule complexes in which the excess negative charges are largely localized on sub-ions within the larger cluster anions. The spectra of $(CO_2)_2^-$, $(SO_2)_2^-$ and $(NO)_2^-$, on the other hand, suggest that these species are somewhat more complicated cases, and that they may not be well described as simple ion-molecule complexes. Also, in the case of NH_4^-, evidence is found not only for the ion-molecule complex, $H^-(NH_3)_1$, but also for a higher-energy isomer of tetrahedral geometry. Additional systems studied include negative cluster ions of water and alkali metal cluster anions. The spectra of $(H_2O)_{n=2,6,7,10\div25,30,34,37,40}^-$ and $Ar(H_2O)_{n=2,6,7}^-$ provide the vertical detachment energies for these species. The spectra of $Na_{2\div5,7}^-$, $K_{2\div8}^-$, $Rb_{2\div4}^-$, $Cs_{2,3}^-$, NaK^-, KRb^-, KCs^-, Na_2K^- and K_2Cs^- yield electron affinities as a function of cluster size as well as the electronic-state splittings for their corresponding neutral alkali metal clusters.

2. – Experimental.

Negative-ion photoelectron spectroscopy is conducted by crossing a mass-selected beam of negative ions with a fixed-frequency photon beam and energy analyzing the resultant photodetached electrons. Subtraction of the center-of-mass electron kinetic energy of an observed spectral feature from the photon energy gives the transition energy (the electron binding energy) from an occupied level in the negative ion to an energetically accessible level in the corresponding neutral. Our negative-ion photoelectron spectrometer has been described previously [55]. It is comprised of three main component systems. These are *a*) the beam line along which negative ions are formed, transported and mass-selected, *b*) the high-power argon ion laser operated intracavity in the ion-photon interaction region and *c*) the doubly magnetically shielded, high-resolution hemispherical electron energy analyzer which is located below the plane of the crossed ion and photon beams. The mass selector is a cooled

Colutron 600B Wien filter. This is a $E \times B$ velocity filter with electrostatic shims which compensate for the focusing effects of simple Wien filters. Mass selection allows us to «purify» our starting sample of negative ions before photodetachment and thus to obtain interference-free photoelectron spectra of specific negative ions. This capability is well suited for studies of homologous series of ions such as negative cluster ions.

Beams of negative cluster ions were generated in a supersonic-expansion ion source similar in spirit to that developed by HABERLAND [56]. Figure 1 presents a schematic of our version of this source. In this source a biased filament located just outside the nozzle orifice injects relatively low-energy electrons into the supersonic expansion. Permanent magnets placed near the expansion jet were found to enhance the production of negative ions.

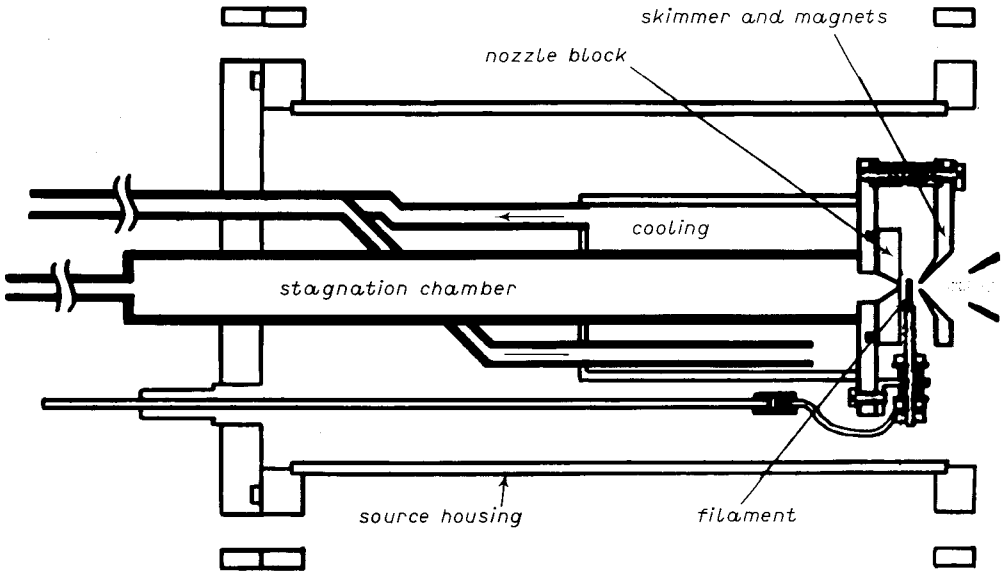

Fig. 1. – Drawing of the supersonic-expansion ion source used in many of these experiments.

3. – Results and discussion.

3·1. *Ion-molecule complexes: cluster anions with localized excess negative charges.*

$NO^-(N_2O)_{n=1\div5}$. The photoelectron (photodetachment) spectra of the gas phase negative cluster ions, $NO^-(N_2O)_{1\div5}$, were recorded using 2.540 eV photons. All of these spectra exhibit structured photoeletron spectral patterns

which strongly resemble that of free NO^-, but which are shifted to successively lower electron kinetic energies with their individual peaks broadened (see fig. 2). Each of these spectra is interpreted in terms of a largely intact NO^- sub-ion which is solvated and stabilized by nitrous oxide molecule(s). The ion-solvent dissociation energies for the loss of a single N_2O solvent molecule from each of

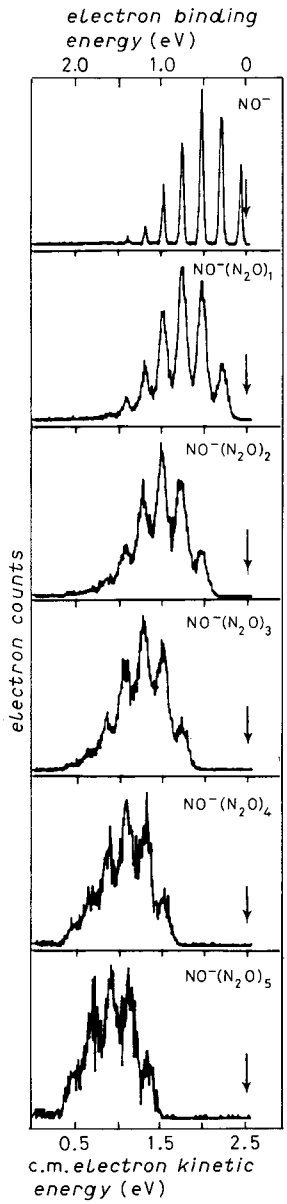

Fig. 2. – The negative-ion photoelectron spectra of NO^- and $NO^-(N_2O)_{n=1\div5}$ all presented on the same center-of-mass electron kinetic energy and electron binding energy scales.

these cluster ions were determined from origin peak shifts to be ~ 0.2 eV each. The total solvation energy thus increased linearly with cluster size, and the electron affinities of these clusters were found to increase smoothly with size. The localization of the cluster ion's excess negative charge onto its nitric oxide rather than its nitrous oxide subunit was interpreted in terms of kinetic factors and a possible barrier between the two forms of the solvated ion [52].

$H^-(NH_3)_{n=1,2}$. The gas phase $H^-(NH_3)_1$ ion was first observed by NIBBERING [57] in a FT-ICR spectrometer. Theoretical calculations by ROSMUS, by RITCHIE, by SQUIRES, by SCHLEYER, by CREMER, by CARDY, by HIRAO and by ORTIZ all agree that the hydride ion is bound at a relatively long distance to only one of ammonia's hydrogens in the most stable configuration of the $H^-(NH_3)_1$ ion-dipole complex, and that $H^-(NH_3)_1$ is more stable than $NH_2^-(H_2)_1$. These calculations found global minima for $H^-(NH_3)_1$ in which the H^- ion lies almost in line with a N-H bond in ammonia. Most of them also found values for the dissociation energy of $H^-(NH_3)_1$ into $H^- + NH_3$ that ranged around about a third of an eV.

In this work, $H^-(NH_3)_{n=1,2}$ ions were generated from ammonia in a

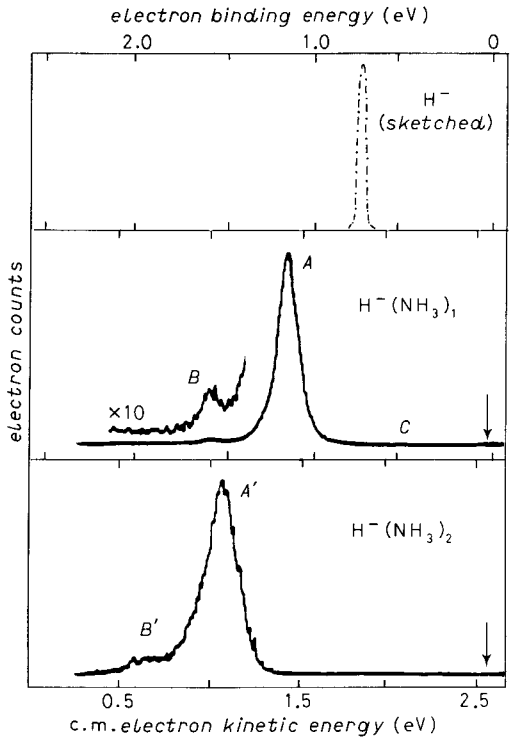

Fig. 3. – The photoelectron spectra of $H^-(NH_3)_1$ and $H^-(NH_3)_2$. The spectrum of $H^-(NH_3)_1$ also shows a $\times 10$ magnified trace.

supersonic-expansion ion source and photodetached with 2.540 eV photons [50]. No homologous series in $NH_2^-(H_2)_n$ was observed. The photoelectron spectra of $H^-(NH_3)_1$ and $H^-(NH_3)_2$ are both dominated by large peaks which we have designated as peaks A and A', respectively, in fig. 3. The $H^-(NH_3)_1$ spectrum also exhibits a smaller peak on the low-electron-kinetic-energy side of peak A which we have labelled peak B. The shoulder on the low-electron-kinetic-energy side of peak A' in the $H^-(NH_3)_2$ spectrum is marked in fig. 3 as peak B'. A much smaller third peak (peak C) also exists in the $H^-(NH_3)_1$ spectrum. This will be discussed in a separate section below.

Our interpretation of peak A in the $H^-(NH_3)_1$ spectrum and of peak A' in the $H^-(NH_3)_2$ spectrum is that they contain the origins of their respective photodetachment transitions. Both peaks are due to the photodetachment of solvated hydride ion «chromophores» within $H^-(NH_3)_1$ and $H^-(NH_3)_2$. This results in the main features (peaks A and A') of the $H^-(NH_3)_1$ and $H^-(NH_3)_2$ photoelectron spectra resembling the photoelectron spectrum of free H^- (a single peak) except for being broadened and *shifted* to lower electron kinetic energies due to the stabilizing effect of solvation.

The electron binding energy of peak A is 1.11 eV. This is interpreted as an upper limit to the energy difference between the lower vibrational states of $H^-(NH_3)_1$ and the $H + NH_3 + e^-$ dissociation asymptote. This value is thus a reasonably close approximation to the dissociative detachment energy of $H^-(NH_3)_1$ (and to the electron affinity of $H(NH_3)$). The electron binding energy of peak A' is 1.46 eV, and it is similarly interpreted. An upper limit to the ion-solvent dissociation energy of $H^-(NH_3)_1$ into H^- and NH_3 (the gas phase solvation energy) is given by subtracting the electron affinity of H (0.754 eV) from the value we have obtained for the upper limit to the dissociative detachment energy of $H^-(NH_3)_1$, *i.e.* the origin peak shift. This value is 0.36 eV, and it is in good agreement with theoretical calculations. Likewise, the ion-solvent dissociation energy of $H^-(NH_3)_2$ into $H^-(NH_3)_1$ and NH_3 is given by subtracting the dissociative detachment energy of $H^-(NH_3)_1$ from that of $H^-(NH_3)_2$, *i.e.* the shift between these origin peaks. This value is 0.35 eV.

Our interpretation of peak B is that it is primarily due to the excitation of a stretching mode (or modes) in the ammonia solvent during photodetachment. The small Franck-Condon factor observed suggests that the ammonia solvent is only slightly distorted by its complexation with H^-. The center of peak B is separated from that of peak A by $(3480 \pm 60)\,cm^{-1}$ in the $H^-(NH_3)_1$ spectrum, and in the $D^-(ND_3)_1$ spectrum the separation between the centers of peaks A and B is $(2470 \pm 80)\,cm^{-1}$. These peak separations are close to the observed stretching frequencies of NH_3 and ND_3, and they, therefore, support our interpretation. The B' shoulder in the spectrum of $H^-(NH_3)_2$ is probably due to analogous transitions. Taken together, the foregoing provides spectroscopic evidence for cluster ions consisting of *intact* hydride ions which are perturbed and solvated by ammonia.

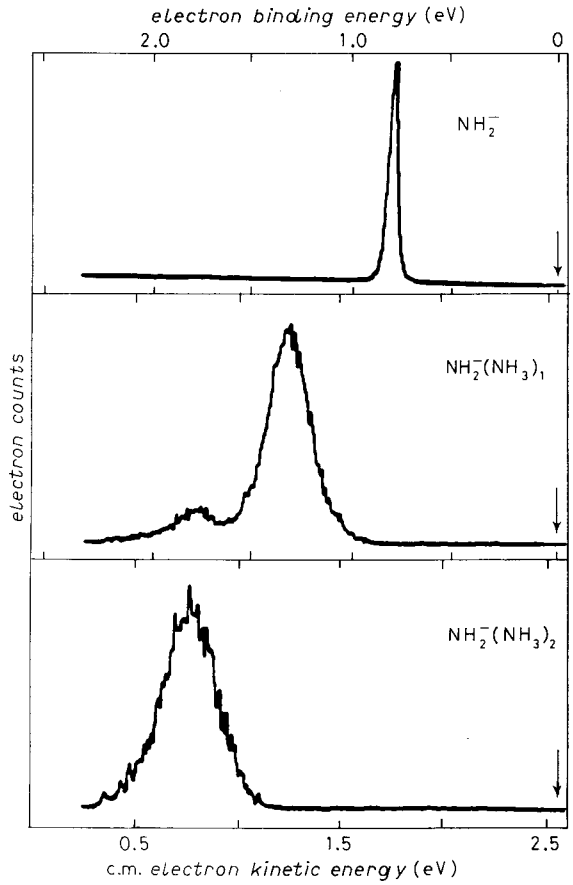

Fig. 4. – The photoelectron spectra of NH_2^-, $NH_2^-(NH_3)_1$ and $NH_2^-(NH_3)_2$ all recorded with 2.540 eV photons.

$NH_2^-(NH_3)_{n=1,2}$. Figure 4 presents the photoelectron spectra of NH_2^-, $NH_2^-(NH_3)_1$, $NH_2^-(NH_3)_2$ all plotted on a common center-of-mass electron kinetic-energy scale. The well-known photoelectron spectrum of NH_2^- is dominated by a single peak, and it is presented in fig. 4 for comparative purposes. The spectra of the clustered ions are also dominated by large peaks (A and A'). These shift to lower electron kinetic energies with increasing solvation and are broadened. Our interpretation of peaks A and A' is that they both contain the origins of their respective photodetachment transitions. Both peaks arise due to the photodetachment of solvated amide ion «chromophores» within the $NH_2^-(NH_3)_1$ and $NH_2^-(NH_3)_2$ cluster ions. The spectral shifts are a consequence of the stabilization of the NH_2^- sub-ion due to its interactions with the NH_3 «solvent» molecule(s) in the cluster ions.

The center of peak A in the $NH_2^-(NH_3)_1$ spectrum corresponds to an electron

binding energy of 1.30 eV. This is interpreted as an upper limit to the energy difference between the lower vibrational states of $NH_2^-(NH_3)_1$ and the $NH_2 + NH_3 + e^-$ dissociation asymptote. This value is a close approximation to the dissociative detachment energy of $NH_2^-(NH_3)_1$ and to the electron affinity. The center of peak A' in the $NH_2^-(NH_3)_2$ spectrum corresponds to an electron binding energy of 1.78 eV, and it is similarly interpreted. An upper limit to the ion-solvent dissociation energy of $NH_2^-(NH_3)_1$ into NH_2^- and NH_3 (the gas phase solvation energy) is given by the magnitude of the shift between the centers of the peak in the NH_2^- spectrum and peak A in the $NH_2^-(NH_3)_1$ spectrum. This is equivalent to subtracting our measured value for the electron affinity of NH_2 from the value of the upper limit to the dissociative detachment energy of $NH_2^-(NH_3)_1$. This value is 0.52 eV, and it is in good agreement with theoretical calculations by SQUIRES. Likewise, the ion-solvent dissociation energy of $NH_2^-(NH_3)_2$ into $NH_2^-(NH_3)_1$ and NH_3 is given by the shift between the centers of peaks A and A' in the cluster ion spectra. This value is 0.48 eV, indicating an approximately equal stabilization of NH_2^- by both the first and the second NH_3 «solvent» molecules.

A less intense peak, designated as peak B, appears on the low-electron-kinetic-energy side of peak A in the photoelectron spectrum of $NH_2^-(NH_3)_1$. The separation between the centers of peaks A and B is close to the observed values of the stretching frequencies of ammonia. Our interpretation of this peak is that it is primarily due to the excitation of a stretching mode (or modes) in the NH_3 solvent during photodetachment. The photoelectron spectrum of $ND_2^-(ND_3)_1$ offers further support of this interpretation. Peak A occurs at essentially the same location in the spectra of $ND_2^-(ND_3)_1$ and $NH_2^-(NH_3)_1$. The spacing between peaks A and B in the spectrum of $ND_2^-(ND_3)_1$, however, has decreased to an energy which is equal to the values of the observed stretching frequencies of ND_3.

As discussed above, we have also studied the species $H^-(NH_3)_1$ and $H^-(NH_3)_2$. *Qualitatively* the photoelectron spectra of $NH_2^-(NH_3)_{n=1,2}$ and $H^-(NH_3)_{n=1,2}$ are rather similar. Both sets of spectra exhibit large peaks (A and A' peaks). Both $H^-(NH_3)_1$ and $NH_2^-(NH_3)_1$ spectra have B peaks to the low-electron-energy side of their A peaks which are separated from them by energies corresponding to that of ammonia's stretching frequencies. *Quantitatively*, however, the $NH_2^-(NH_3)_{n=1,2}$ spectra exhibit larger shifts and more broadening than the $H^-(NH_3)_{n=1,2}$ spectra. We have found that the first and second ion-solvent dissociation energies for $NH_2^-(NH_3)_1$ and $NH_2^-(NH_3)_2$ are both ~ 0.5 eV, while those for $H^-(NH_3)_1$ and $H^-(NH_3)_2$ are both ~ 0.36 eV. Clearly, the interaction of NH_2^- with ammonia is stronger than that of H^- with ammonia. Calculations by SQUIRES find that $H^-(NH_3)_1$ and $NH_2^-(NH_3)_1$ have similar gross structures. Using flowing afterglow techniques to study the $NH_2^- + H_2 \rightarrow$ $\rightarrow H^- + NH_3$ reaction, BOHME has shown that NH_2^- is a stronger base than H^- in the gas phase. It thus seems likely that the higher ion-solvent dissociation

energy of $NH_2^-(NH_3)_1$ relative to that of $H^-(NH_3)_1$ is a consequence of NH_2^- being a stronger base than H^-.

The clustering of solvent molecules around a bare gas phase anion stabilizes the excess negative charge on the ion, and this results in a decrease in the gas phase basicity. It is often the case, in fact, that the ordering of basicities in the gas phase is the reverse of their ordering in solution. Using our results to calculate the relative basicites of NH_2^- *vs.* H^-, $NH_2^-(NH_3)_1$ *vs.* $H^-(NH_3)_1$ and $NH_2^-(NH_3)_2$ *vs.* $H^-(NH_3)_2$ shows that such a reversal in the ordering of basicities in these systems occurs by the addition of a second ammonia solvent to NH_2^- and to H^-. This illustrates the role that cluster ions can play in illuminating the size regime between the gaseous and the condensed (solution) phase.

Both $NH_2^-(NH_3)_1$ and $H^-(NH_3)_1$ spectra show an *A*-*B* peak spacing that is indicative of an ammonia stretching frequency. The relative intensity of the *B* peak in each of these spectra is a measure of the degree to which the ammonia «solvent» molecule is distorted due to its complexation with the anion. This peak is larger in the $NH_2^-(NH_3)_1$ spectrum than in the $H^-(NH_3)_1$ spectrum, and this is consistent with the stronger interaction implied by the larger ion-solvent bond dissociation energy found for $NH_2^-(NH_3)_1$. These observations are also consistent with calculations by SQUIRES. He finds that the ammonia N-H bond which interacts with the anion is more elongated in $NH_2^-(NH_3)_1$ than in $H^-(NH_3)_1$.

$NO^-(Ar)_1$, $NO^-(Kr)$ and $NO^-(Xe)_1$. The photoelectron spectra of $NO^-(Ar)_1$, $NO^-(Kr)_1$ and $NO^-(Xe)_1$ were recorded with 2.409 eV photons. All of these rare-gas (Rg) negative-cluster-ion spectra exhibit structured spectral patterns which strongly resemble that obtained for free NO^-, but which are shifted to lower electron energies with their individual peaks broadened (see fig. 5). Each of these spectra is interpreted in terms of a largely intact NO^- sub-ion which is solvated and stabilized by its rare-gas solvent atom. The ion-solvent dissociation energy for a given $NO^-(Rg)_1$ cluster ion dissociating into NO^- and Rg is approximately given by the energy difference between the origin peak of the free-NO^- spectrum and the origin peak of a given $NO^-(Rg)_1$ spectrum. The values of these shifts were found to be (0.058 ± 0.011) eV, (0.099 ± 0.018) eV and (0.161 ± 0.024) eV for the argon, krypton and xenon complexes, respectively. A plot of these energy shifts *vs.* the polarizabilities of the rare-gas atoms gave a straight line. Values for the electron affinities of these complexes were found to be 0.095 eV, 0.136 eV and 0.204 eV for the argon, krypton and xenon complexes, respectively.

$O_2^-(Ar)_1$. The photoelectron spectrum of $O_2^-(Ar)_1$ exhibits the highly structured photoelectron spectral pattern of free O_2^- shifted to lower electron kinetic energy by ~ 70 meV, the ion-atom dissociation energy of this anion-atom complex.

$NO^-(H_2O)_{n=1,2}$. The photoelectron spectra of $NO^-(H_2O)_{n=1,2}$ and their deuterated analogs were recorded with 2.540 eV photons. Even though these

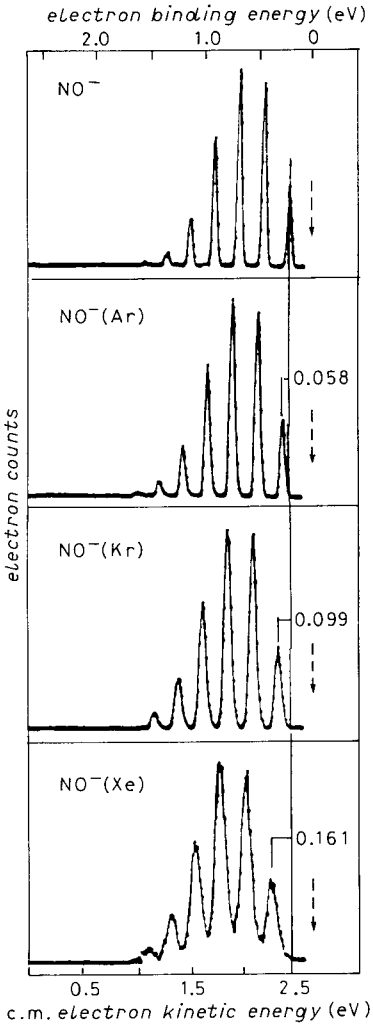

Fig. 5. The photoelectron spectra of NO^-, $NO^-(Ar)_1$, $NO^-(Kr)_1$ and $NO^-(Xe)_1$.

spectra were essentially unstructured, the gross envelope of the NO^- spectral pattern was retained in each. The ion-solvent dissociation energy for $NO^-(H_2O)_1$ was found to be 0.72 eV, while the dissociation energy for losing a single water molecule from $NO^-(H_2O)_2$ was determined to be 0.68 eV. These are among the largest solvation energies that we have encountered thus far, and they doubtless arise due to strong ion-dipole plus hydrogen bonding interactions between the NO^- sub-ion and its water solvent molecule(s).

$(N_2O)^-_{n=1,2}$. The photoelectron spectra of N_2O^- and $(N_2O)_2^-$ were recorded with 2.540 eV photons [51] (see fig. 6). Because of the large geometrical difference

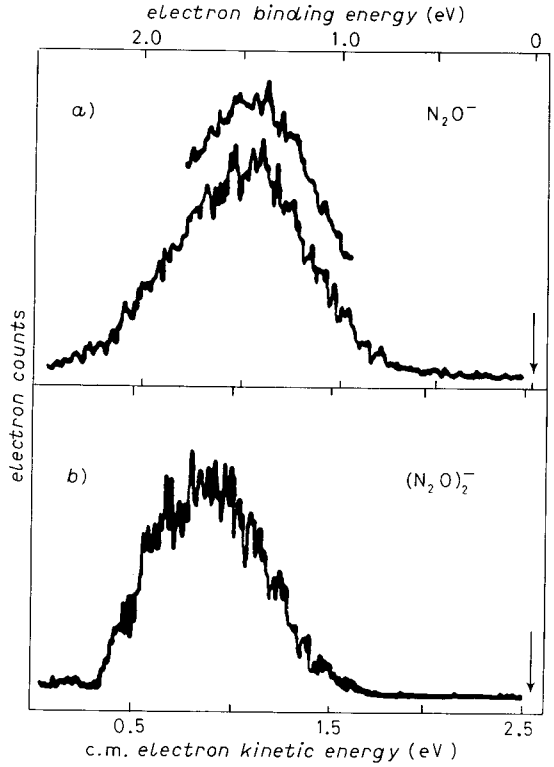

Fig. 6. – The photoelectron spectrum of *a*) N_2O^- and *b*) $(N_2O)_2^-$ presented on aligned center-of-mass electron kinetic energy and electron binding energy scales. Both spectra were recorded with 2.540 eV photons. The limited range scan above the full spectrum of N_2O^- has 2.5 times more signal.

between N_2O (linear) and N_2O^- (bent), there is little Franck-Condon overlap between the lowest-lying levels in the ion and its neutral. We interpret the photoelectron spectrum of N_2O^- as being largely due to an unresolved progression in the bending mode of N_2O. The electron binding energy corresponding to the maximum in the N_2O^- spectrum is ~ 1.5 eV and is a good measure of the vertical detachment energy of N_2O^-. The spectrum of $(N_2O)_2^-$ provides information on the distribution of excess charge within the negative dimer ion. The maximum in the $(N_2O)_2^-$ spectrum is shifted by 0.19 eV to lower electron kinetic energy relative to the maximum in the N_2O^- spectrum. We interpret the $(N_2O)_2^-$ spectrum as arising from the photodetachment of an ionic species which is best described as a bent N_2O^- solvated by a neutral linear N_2O, *i.e.* as $N_2O^-(N_2O)_1$ and the ~ 0.2 eV shift between the N_2O^- and the $(N_2O)_2^-$ spectra as a measure of the dimer anion's dissociation energy into N_2O^- and N_2O.

$(CS_2)_2^-$. In addition to nitrous oxide, carbon disulfide and carbon dioxide are also linear triatomic molecules with bent anions. The photoelectron spectrum of

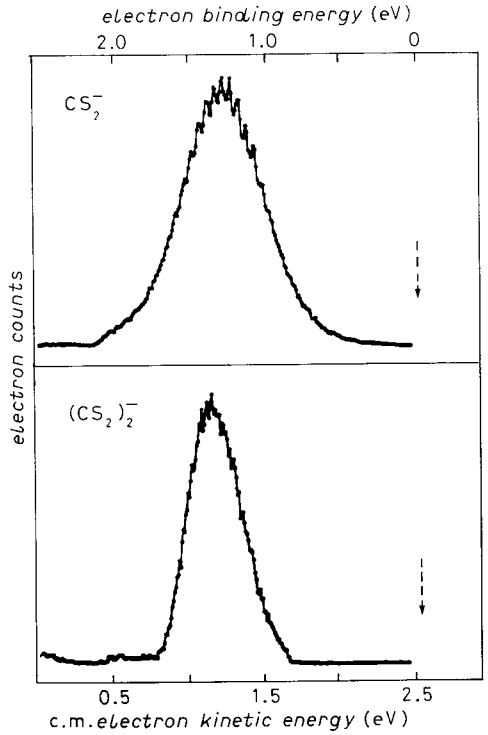

Fig. 7. – The photoelectron spectra of CS_2^- and $(CS_2)_2^-$. Both spectra were taken using 2.540 eV photons.

$(CS_2)_2^-$ bears a substantial resemblance to that of the monomeric ion CS_2^- (ref. [58]), except for the former being shifted to lower electron kinetic energies relative to the latter (see fig. 7). Our interpretation of the $(CS_2)_2^-$ spectrum leads to the conclusion that $(CS_2)_2^-$ is composed of a largely intact CS_2^- ion which is «solvated» by a neutral CS_2, *i.e.* the dimer ion is an ion-neutral complex. We have determined the ion-solvent dissociation energy for the dimer ion dissociating into CS_2^- and CS_2 to be (0.176 ± 0.025) eV.

3·2. *More complicated cases: cluster anions with excess charge dispersal.*

$(CO_2)_{n=1,2}^-$. The photoelectron spectra of CO_2^- and $(CO_2)_2^-$, which were both recorded with 2.540 eV photons, are presented in fig. 8. Unlike N_2O and CS_2, CO_2 has a negative adiabatic electron affinity. The negative ion, CO_2^-, is thus metastable and has an autodetachment lifetime of 90 μs. Because of the relative energies and large geometrical differences between CO_2 and CO_2^-, there should be little if any Franck-Condon overlap between the lowest-lying levels of the ion and its neutral. We interpret the photoelectron spectrum of CO_2^- as being largely due to a progression in the bending mode of CO_2. The structure near the

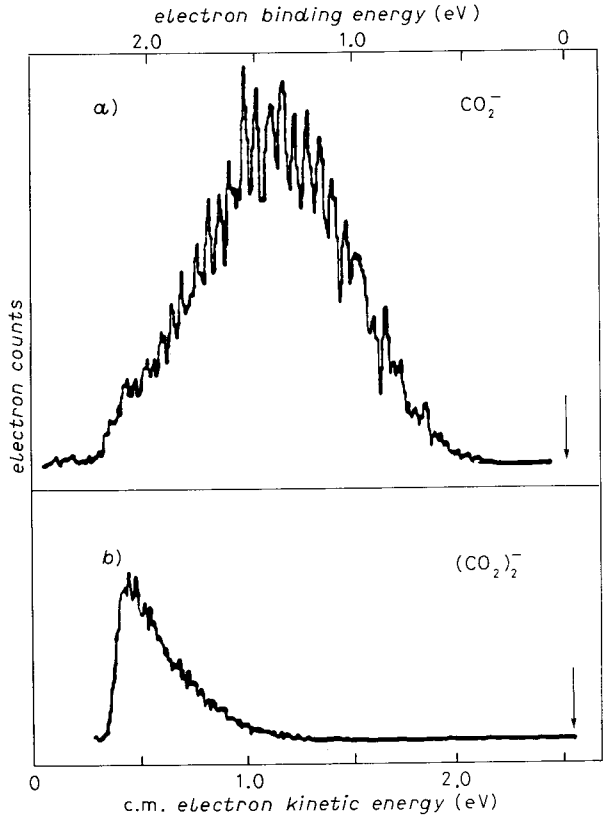

Fig. 8. – The photoelectron spectra of CO_2^- and $(CO_2)_2^-$.

maximum of the CO_2^- spectrum is real, and the peak spacings probably correspond to the energy differences between anharmonic bending levels in CO_2. The electron binding energy corresponding to the maximum in our CO_2^- spectrum is interpreted to be the vertical detachment energy of CO_2^-. This value, 1.4 eV, is in good agreement with Jordan's calculated value for the vertical detachment energy of CO_2^-. The photoelectron spectrum of $(CO_2)_2^-$ is presented in fig. 8. The downward turn on the low-electron-kinetic-energy side of this spectrum is an experimental artifact due to the rapid and unavoidable decrease in the transmission functions of electron energy analyzers at low electron kinetic energies. Spectra taken with 2.707 eV photons show that the photodetachment cross-section is still increasing at the false maximum in the 2.540 eV spectrum. Thus with visible photons the spectrum of $(CO_2)_2^-$ exhibits only the lower-energy photodetachment transitions of $(CO_2)_2^-$. Assuming that there is a spectral maximum in the $(CO_2)_2^-$ spectrum, it must occur at an electron binding energy that is >2.4 eV, *i.e.* the maximum in the $(CO_2)_2^-$ spectrum is shifted to lower electron kinetic energies by >1 eV with respect to the maximum

in the CO_2^- spectrum. This suggests that there is a substantial difference between $(CO_2)_2^-$ and $(N_2O)_2^-$ and $(CS_2)_2^-$. Recent calculations by JORDAN on the various possible structures for $(CO_2)_2^-$ shed substantial light on this problem. Upon re-examining the relative energies of the symmetrical D_{2d} form of $C_2O_4^-$ and the asymmetrical ion-molecule complex, JORDAN found the former to be more stable by ~ 0.2 eV. More importantly, however, he also found that these two forms of the anion gave rather different vertical detachment energies and that the calculated VDE for the D_{2d} form is consistent with our measurements. Thus it appears that even though $(N_2O)_2^-$ and $(CS_2)_2^-$ are ion-molecule complexes, $(CO_2)_2^-$ is not. Perhaps, it is better described as $C_2O_4^-$.

$NH_4^-(T_d)$. As mentioned earlier, the photoelectron spectrum of NH_4^- is dominated by two peaks (A and B) which arise due to the photodetachment of electrons from the ion-molecule complex, $H^-(NH_3)_1$. In addition, however, there is also a much smaller third peak (C) in the spectrum, and this feature provides the first experimental evidence for a higher-energy isomer of NH_4^- of tetrahedral geometry. Figure 9 shows magnified traces of peak C in both the $H^-(NH_3)_1$ and the $D^-(ND_3)_1$ spectra. Since negative ions in this experiment are carefully mass-selected before photodetachment, the existence of peak C in both of these

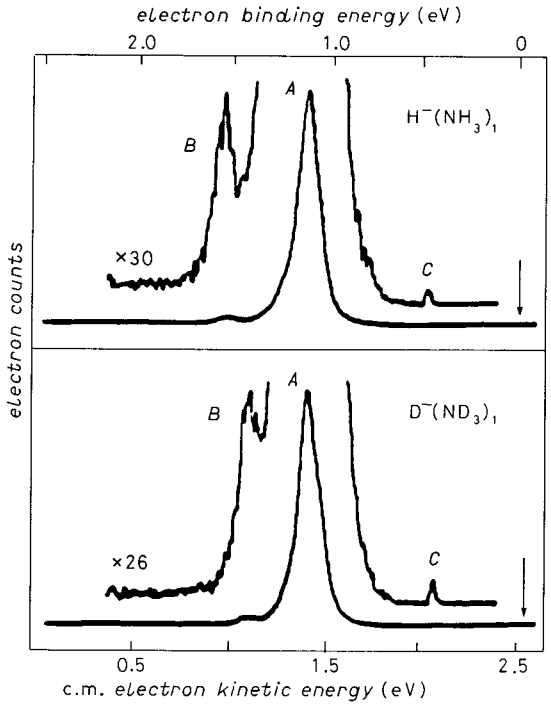

Fig. 9. – The photoelectron spectra of NH_4^- and ND_4^- showing features due to both the ion-molecule complexes (peaks A and B) and the tetrahedral isomer (peak C).

spectra is good evidence that it is not due to an «impurity» ion. Peak C occurs at too high of an electron kinetic energy to be due to NH_2^- (or to OH^-). Since clustering is expected to stabilize the excess negative charge on an anion and to shift spectral features toward lower (rather than higher) electron energies, it is also unlikely that peak C is due to the presence of small amounts of $NH_2^-(H_2)_1$. The photodissociation of $H^-(NH_3)_1$ into $H^- + NH_3$ followed by the photodetachment of electrons from the nascent H^- is a two-step process which is energetically accessible with 2.5 eV photons. If this process were to occur, however, it would result in electrons with kinetic energies substantially lower than that of peak C (possible kinematic effects having been carefully considered). In addition, the laser power dependence of peak C's intensity is linear, and, while not proof in itself, this is consistent with a single-photon process. Further insight into the possible origin of peak C derives from its intensity variation with source conditions and from its behavior in the spectrum of the deuterated cluster ion $D^-(ND_3)_1$. While the relative intensities of peaks A and B are essentially constant as source conditions are varied, the relative intensity of peak C changes substantially from day to day. Such intensity variations are indicative of photodetachment transitions which originate from an excited state of the ion and they are often associated with vibrationally excited negative-ion states. Hot-band peaks arising from such transitions, however, should shift with deuteration, and peak C does not. Peak C behaves as if it arises from the photodetachment of an electronically higher-energy form of the negative ion. It seems unlikely that peak C is due to the photodetachment of an electronically excited state of $H^-(NH_3)_1$. Our observations are consistent with it being due to the photodetachment of a higher-energy isomer of an ion with molecular formula NH_4^-. The width of peak C is quite narrow, much narrower than peaks A and B. This implies that the structure of the ion being photodetached and the equilibrium structure of its corresponding neutral are rather similar. Neutral NH_4 is known to have a tetrahedral configuration. This suggests that the form of NH_4^- that gives rise to peak C is also of tetrahedral geometry. Also, the united atom for NH_4 is Na. The electron affinity of Na is ~ 0.5 eV. The electron binding energy of the species that gives rise to peak C is ~ 0.5 eV. In addition, calculations by SCHLEYER, by CREMER, by CARDY and by ORTIZ all find a higher-energy isomer of NH_4^- of tetrahedral geometry. The energy of $NH_4^-(T_d)$ above the global minima of $H^-(NH_3)_1$ is also consistent with our spectra. It seems likely that $NH_4^-(T_d)$ should be envisioned as an NH_4^+ core with two Rydberg-like electrons around it. Thus NH_4^+, NH_4 and NH_4^- can all exist in tetrahedral forms. Moreover, they are all really the same thing, *i.e.* NH_4^+ cores with 0, 1 and 2 loose electrons associated with them.

$(SO_2)_2^-$ and $(NO)_2^-$. The photoelectron spectra of $(SO_2)_2^-$ and of $(NO)_2^-$ do not show the shifted «fingerprint» spectral patterns of SO_2^- and of NO^- that one might expect of *simple*, localized excess charge ion-molecule complexes, *i.e.* of

$SO_2^-(SO_2)_1$ and of $NO^-(NO)$. The component parts of these dimer ions may resonantly share the excess electron. This appears likely in the case of $(SO_2)_2^-$ where the observed spectral shift between the origin peak of the SO_2^- spectrum and the suspected origin in the $(SO_2)_2^-$ spectrum implies an ion-solvent dissociation energy that is reasonable for an ion-molecule complex. The spectrum of $(NO)_2^-$, on the other hand, implies a lower limit to its electron affinity of ~ 2.1 eV. This implies that $(NO)_2^-$ enjoys a high degree of electron dispersal, and that it may be better described as the unclustered ion, $N_2O_2^-$. Studies by JOHNSON [29] at higher photon energies indicate the existence of other isomers of $N_2O_2^-$ as well.

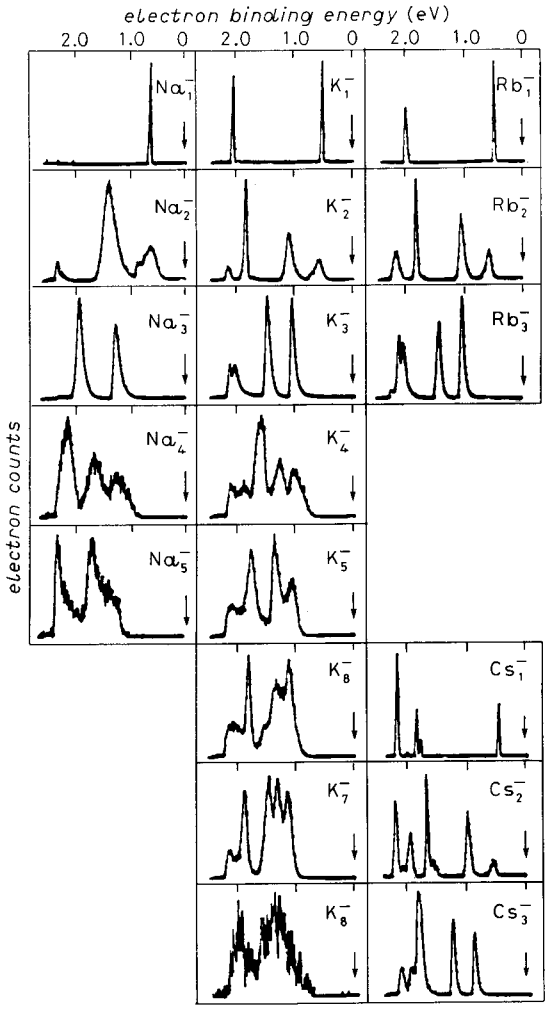

Fig. 10. – The photoelectron spectra of the homogeneous alkali metal cluster anions $Na_{2\div5}^-$, $K_{2\div8}^-$, $Rb_{2,3}^-$ and $Cs_{2,3}^-$.

3·3. *Alkali metal cluster anions.* – The study of metal clusters provides an avenue for exploring the variation in the electronic properties of metals in the transition size regime between atoms and the solid-state bulk. For metals, properties such as ionization potentials and electron affinities typically vary in magnitude by several eV from their atomic to their bulk (work function) values. Presumably, clusters of intermediate size have electronic properties with intermediate values. For phenomena where the properties of matter in the

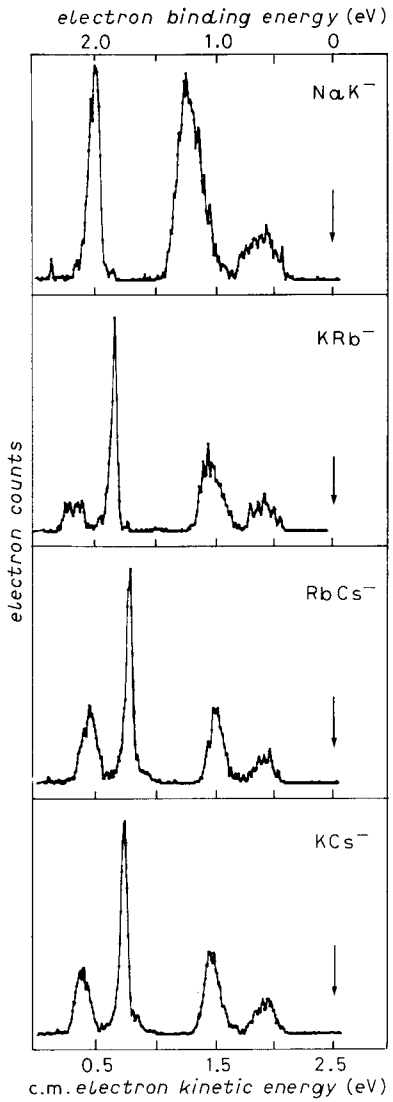

Fig. 11. – The photoelectron spectra of the heterogeneous alkali metal dimer anions NaK^-, KRb^-, $RbCs^-$ and KCs^-.

regime of small sizes are important, *e.g.* surface reactivity and thin films, these variations in electronic properties can have pivotal effects. In principle, the study of the electronic properties of metal clusters as a function of cluster size could allow us to observe the evolution of the electronic states of metals from those of their atoms toward those of band theory.

The alkali metals are the simplest of metals. Using 2.540 eV photons we have recently recorded the photoelectron spectra of the homogeneous alkali cluster anions $Na^-_{n=2\div5,7}$, $K^-_{n=2\div8}$, $Rb^-_{n=2\div4}$ and $Cs^-_{n=2,3}$ (see fig. 10) and the heterogeneous alkali dimer and trimer anions NaK^-, KRb^-, $RbCs^-$, KCs^- (see fig. 11), Na_2K^- and K_2Cs^-. These highly structured spectra map out both the electron affinities *vs.* cluster size for those cluster anions studied thus far and the electronic-state splittings of their corresponding *neutral* clusters (at the geometry of their cluster anions) *vs.* cluster size. The dimer anion spectra have been completely assigned. These provide adiabatic electron affinities, vertical detachment energies, dimer anion dissociation energies, neutral-dimer electronic-state

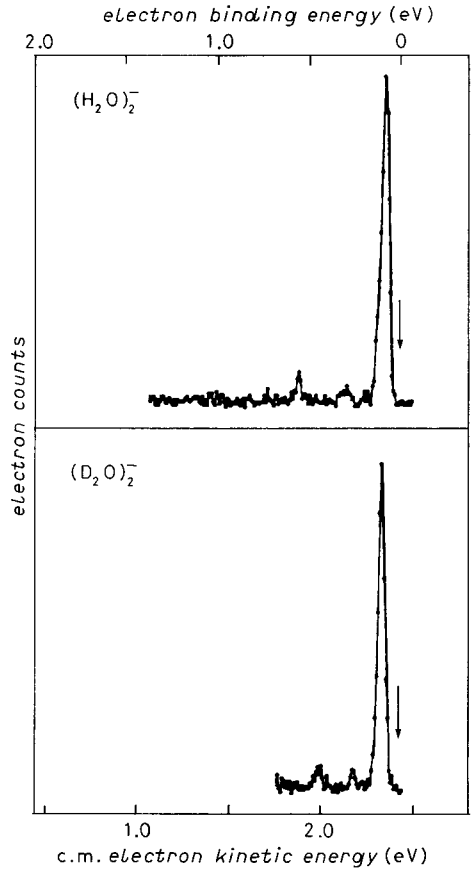

Fig. 12. – The photoelectron spectra of $(H_2O)_2^-$ and $(D_2O)_2^-$.

spacings and bond lengths for the various excited electronic states of the neutral dimers. Thus far, we have obtained our most complete set of data on potassium cluster anions. Potassium ([Ar]$4s^1$) should be electronically analogous to copper ([Ar]$3d^{10}4s^1$). A comparison of the electron affinity *vs.* cluster size trends for potassium clusters with those for copper clusters (measured by LINEBERGER [45] and by SMALLEY [23]) of the same size shows quantitative differences (copper has a substantially larger work function) yet strikingly similar *qualitative* trends. Most of the structure in these spectra comes about due to the electronic states of the neutral clusters. One can see qualitative similarities between the UV photodetachment spectra of copper cluster anions and our visible spectra of potassium cluster anions. This correlation with the UV experiments is reasonable, since the electronic states of neutral copper clusters might be expected to be more widely spaced in energy than those of neutral potassium clusters.

3·4. *Water cluster anions.* – Over the years, it has often been suggested that gas phase $(H_2O)_n^-$ cluster ions ought to exist and that they might be the gas phase counterparts to condensed-phase solvated (hydrated) electrons. A few years

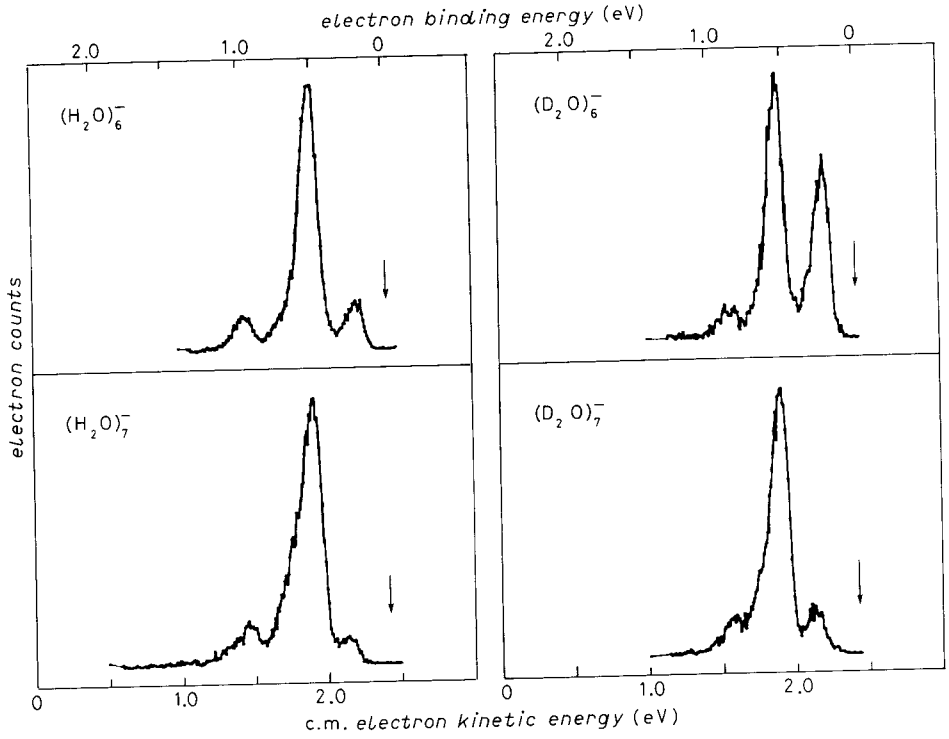

Fig. 13. – The photoelectron spectra of $(H_2O)_{6,7}^-$ and $(D_2O)_{6,7}^-$.

es of the neutral
ata on potassium
logous to copper
r size trends for
(measured by
ows quantitative
) yet strikingly
tra comes about
see qualitative
er cluster anions
tion with the UV
l copper clusters
those of neutral

n suggested that
be the gas phase
as. A few years

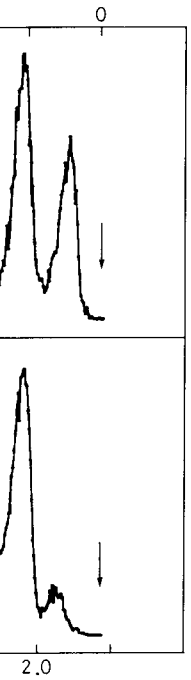

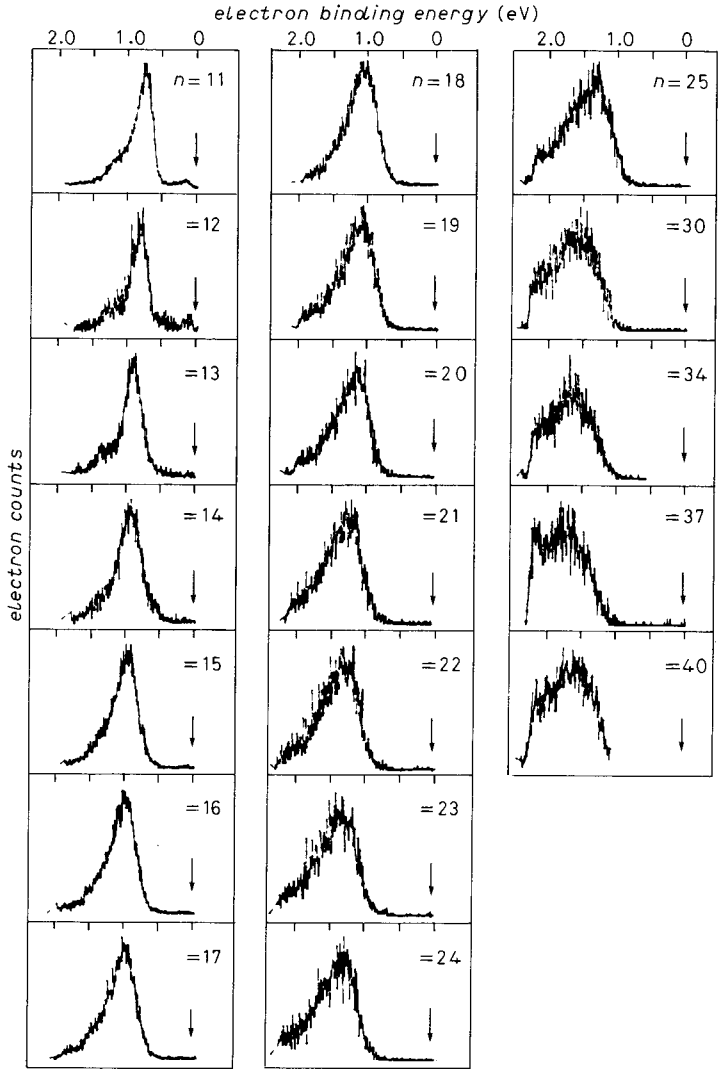

Fig. 14. – The photoelectron spectra of $(H_2O)^-_{n=11\div25,30,34,37,40}$.

ago, these entities were observed for the first time in the gas phase by HABERLAND.

Following these developments, we generated $(H_2O)^-_{n=11\div21}$ from neat water expansions in a supersonic-expansion ion source and recorded the photoelectron spectra of $(H_2O)^-_{n=11\div15,19}$ using 2.409 eV photons [59]. Each of these spectra consists of a single broadened peak, and these are shifted to successively lower electron kinetic energies with increasing cluster ion size. We interpreted the electron binding energies of the fitted centers of these spectral peaks to

correspond to the vertical detachment energies for each of the cluster anions. These vertical detachment energies vary smoothly from 0.75 eV for $(H_2O)_{11}^-$ to 1.12 eV for $(H_2O)_{19}^-$. More recently, we have collaborated with HABERLAND and his student, C. LUDEWIGT, to photodetach more water cluster anions. At this point the list of water cluster anions that we have photodetached includes $(H_2O)_{n=2,6,7,10\div25,30,34,37,40}^-$, $(D_2O)_{n=2,6,7,11\div23}^-$, $Ar(H_2O)_{n=2,6,7}^-$, $Ar(D_2O)_{n=2,6,7}^-$ and $Ar_2(D_2O)_6^-$. The dimer anion spectra are presented in fig. 12, the spectra for $(H_2O)_{6,7}^-$ and $(D_2O)_{6,7}^-$ in fig. 13 and the spectra for $(H_2O)_{n=11\div25,30,34,37,40}^-$ in fig. 14.

The spectrum of the water dimer anion is particularly interesting. Calculations have generally predicted the structure of $(H_2O)_2^-$ to be the same as that of $(H_2O)_2$, *i.e.* the excess electron was not found to distort the structure of neutral water dimer. In the spectrum of $(H_2O)_2^-$, however, we observe peak spacings which are characteristic of H_2O bending and stretching frequencies. In the $(D_2O)_2^-$ spectrum, we see these spacings shift appropriately for a D_2O bend and a D_2O stretch. Thus it is clear that at least one water component within the water dimer anion is slightly distorted. We also measure the vertical detachment energy to be ~ 47 meV for water dimer anion. Since there is some structural difference between the anion and its neutral, the adiabatic electron affinity of water dimer should be a little less than 47 meV.

* * *

This research was supported by the National Science Foundation under Grant No. CHE-8511320. Some of the work on the negative cluster ions of water was performed in collaboration with H. HABERLAND, C. LUDEWIGT and D. WORSNOP, and it was partially supported by a NATO Collaborative Research Grant (# 86/307).

REFERENCES

[1] P. KEBARLE: *Ion-Molecule Reactions*, edited by J. L. FRANKLIN (Plenum, New York, N.Y., 1972).
[2] R. G. KEESEE and A. W. CASTLEMAN jr.: *J. Phys. Chem. Ref. Data*, **15**, 1011 (1986).
[3] R. G. KEESEE, N. LEE and A. W. CASTLEMAN jr.: *J. Chem. Phys.*, **73**, 2195 (1980).
[4] D. L. ALBRITTON: *At. Data Nucl. Data Tables*, **22** (1978).
[5] C. E. KLOTS and R. N. COMPTON: *J. Chem. Phys.*, **69**, 1636 (1978).
[6] K. H. BOWEN, G. W. LIESEGANG, R. A. SANDERS and D. R. HERSCHBACH: *J. Phys. Chem.*, **87**, 557 (1983).
[7] P. C. COSBY, J. H. LING, J. R. PETERSON and J. T. MOSELEY: *J. Chem. Phys.*, **65**, 5267 (1976).
[8] R. A. BEYER and J. A. VANDERHOFF: *J. Chem. Phys.*, **65**, 2313 (1976).
[9] A. W. CASTLEMAN jr., D. E. HUNTON, T. G. LINDEMAN and D. N. LINDSAY: *Int. J. Mass Spectrom. Ion Phys.*, **47**, 199 (1983).
[10] H.-S. KIM and M. BOWERS: *J. Chem. Phys.*, **85**, 2718 (1986).

[11] S. GOLUB and B. STEINER: *J. Chem. Phys.*, **49**, 5191 (1968).
[12] H. KISTENMACHER, H. POPKIE and E. CLEMENTI: *J. Chem. Phys.*, **61**, 5627 (1973).
[13] G. CHALASINSKI, R. A. KENDALL and J. SIMONS: *J. Phys. Chem.*, **91**, 6151 (1987).
[14] S. H. FLEISHMAN and K. D. JORDAN: *J. Phys. Chem.*, **91**, 1300 (1987).
[15] R. N. BARNETT, U. LANDMAN, C. L. CLEVELAND and J. JORTNER: *J. Chem. Phys.*, 88, 4429 (1988).
[16] M. D. NEWTON: *J. Phys. Chem.*, **79**, 2795 (1975).
[17] J. SIMONS: *Annu. Rev. Phys. Chem.*, **28**, 15 (1977).
[18] C. F. MELIUS, T. H. UPTON and W. A. GODDARD III: *Solid State Commun.*, **28**, 501 (1978).
[19] I. BOUSTANI and J. KOUTECKY: *J. Chem. Phys.*, 88, 5657 (1988).
[20] S. H. YANG, C. L. PETTIETTE, J. CONCEICAO, O. CHESHNOVSKY and R. E. SMALLEY: *Chem. Phys. Lett.*, **139**, 233 (1987).
[21] S. YANG, K. J. TAYLOR, M. J. CRAYCRAFT, J. CONCEICAO, C. L. PETTIETTE, O. CHESHNOVSKY and R. E. SMALLEY: *Chem. Phys. Lett.*, 88, 431 (1988).
[22] L.-S. ZHENG, C. M. KARNER, P. J. BRUCAT, S. H. YANG, C. L. PETTIETTE, M. J. CRAYCRAFT and R. E. SMALLEY: *J. Chem. Phys.*, **85**, 1681 (1986).
[23] C. L. PETTIETTE, S. H. YANG, M. J. CRAYCRAFT, J. CONCEICAO, R. T. LAAKSONEN, O. CHESHNOVSKY and R. E. SMALLEY: *J. Chem. Phys.*, 88, 5377 (1988).
[24] C. L. PETTIETTE and R. E. SMALLEY: private communication.
[25] L.-S. ZHENG, P. J. BRUCAT, C. L. PETTIETTE, S. YANG and R. E. SMALLEY: *J. Chem. Phys.*, 83, 4273 (1985).
[26] Y. LIU, Q.-L. ZHANG, F. K. TITTEL, R. F. CURL and R. E. SMALLEY: *J. Chem. Phys.*, **85**, 7434 (1986).
[27] O. CHESHNOVSKY, S. H. YANG, C. L. PETTIETTE, M. J. CRAYCRAFT, Y. LIU and R. E. SMALLEY: *Chem. Phys. Lett.*, 138, 119 (1987).
[28] L. A. POSEY, M. J. DELUCA and M. A. JOHNSON: *Chem. Phys. Lett.*, **131**, 170 (1986).
[29] L. A. POSEY and M. A. JOHNSON: *J. Chem. Phys.*, 88, 5383 (1988).
[30] M. J. DELUCA, B. LIU and M. A. JOHNSON: *J. Chem. Phys.*, 88, 5857 (1988).
[31] M. A. JOHNSON: private communication.
[32] R. B. METZ, T. KITSOPOULOS, A. WEAVER and D. M. NEUMARK: *J. Chem. Phys.*, 88, 1463 (1988).
[33] A. WEAVER, R. B. METZ, S. E. BRADFORTH and D. M. NEUMARK: *J. Phys. Chem.*, **92**, 5558 (1988).
[34] D. M. NEUMARK: private communication.
[35] G. GANTEFOR, K. H. MEIWES-BROER and H. O. LUTZ: *Phys. Rev. A*, in press.
[36] G. GANTEFOR, K. H. MEIWES-BROER and H. O. LUTZ: *Phys. Rev. A*, submitted.
[37] C. R. MOYLAN, J. A. DODD and J. I. BRAUMAN: *Chem. Phys. Lett.*, **118**, 38 (1985).
[38] C. R. MOYLAN, J. A. DODD, C.-C. HAN and J. I. BRAUMAN: *J. Chem. Phys.*, 86, 5350 (1987).
[39] D. M. WETZEL and J. I. BRAUMAN: *Chem. Rev.*, 87, 607 (1987).
[40] P. C. ENGELKING and W. C. LINEBERGER: *J. Am. Chem. Soc.*, **101**, 5569 (1979).
[41] A. E. STEVENS, C. S. FEIGERLE and W. C. LINEBERGER: *J. Am. Chem. Soc.*, **104**, 5026 (1982).
[42] T. M. MILLER, D. G. LEOPOLD, K. K. MURRAY and W. C. LINEBERGER: *Bull. Am. Phys. Soc.*, **30**, 880 (1985).
[43] D. G. LEOPOLD, T. M. MILLER and W. C. LINEBERGER: *J. Am. Chem. Soc.*, **108**, 178 (1986).
[44] D. G. LEOPOLD and W. C. LINEBERGER: *J. Chem. Phys.*, 85, 51 (1986).

[45] D. G. LEOPOLD and W. C. LINEBERGER: *J. Chem. Phys.*, **86**, 1715 (1987).
[46] D. G. LEOPOLD, J. ALMLOF, W. C. LINEBERGER and P. R. TAYLOR: *J. Chem. Phys.*, 88, 3780 (1988).
[47] K. M. ERVIN, J. HO and W. C. LINEBERGER: *J. Chem. Phys.*, submitted.
[48] W. C. LINEBERGER, K. M. ERVIN and D. G. LEOPOLD: private communication.
[49] M. R. NIMLOS, L. B. HARDING and G. B. ELLISON: *J. Chem. Phys.*, 87, 5116 (1987).
[50] J. V. COE, J. T. SNODGRASS, C. B. FREIDHOFF, K. M. MCHUGH and K. H. BOWEN: *J. Chem. Phys.*, **83**, 3169 (1985).
[51] J. V. COE, J. T. SNODGRASS, C. B. FREIDHOFF, K. M. MCHUGH and K. H. BOWEN: *Chem. Phys. Lett.*, **124**, 274 (1986).
[52] J. V. COE, J. T. SNODGRASS, C. B. FREIDHOFF, K. M. MCHUGH and K. H. BOWEN: *J. Chem. Phys.*, 87, 4302 (1987).
[53] J. T. SNODGRASS, J. V. COE, C. B. FREIDHOFF, K. M. MCHUGH and K. H. BOWEN: *J. Chem. Phys.*, 88, 8014 (1988).
[54] K. H. BOWEN and J. G. EATON: in *Proceedings of the International Workshop on the Structure of Small Molecules and Ions*, edited by R. NAAMAN and Z. VAGER (Plenum, Jerusalem, 1988).
[55] J. V. COE, J. T. SNODGRASS, C. B. FREIDHOFF, K. M. MCHUGH and K. H. BOWEN: *J. Chem. Phys.*, 84, 618 (1986).
[56] H. HABERLAND, H.-G. SCHINDLER and D. R. WORSNOP: *Ber. Bunsenges. Phys. Chem.*, 88, 270 (1984).
[57] J. C. KLEINGELD, S. INGEMANN, J. E. JALONEN and N. M. M. NIBBERING: *J. Am. Chem. Soc.*, **105**, 2474 (1983).
[58] J. M. OAKES and G. B. ELLISON: *Tetrahedron*, **42**, 6262 (1986).
[59] J. V. COE, D. WORSNOP and K. H. BOWEN: to be published.